NIH Public Access
Author Manuscript
J Am Chem Soc. Author manuscript; available in PMC 2011 August 4.

Published in final edited form as:
J Am Chem Soc. 2010 August 4; 132(30): 10383–10390. doi:10.1021/ja102252d.

Protein and Small Molecule Recognition Properties of Deep Cavitands in a Supported Lipid Membrane Determined by Calcination-Enhanced SPR Spectroscopy

Ying Liu, **Puhong Liao**, **Quan Cheng***, and **Richard J. Hooley***
Department of Chemistry, University of California, Riverside, CA 92521

Abstract

This report details the incorporation of a water-soluble deep cavitand into a membrane bilayer assembled onto a nanoglassified surface for study of molecular recognition in a membrane-mimicking setting. The cavitand retains its host properties, and real-time analysis of the host:guest properties of the membrane:cavitand complex *via* surface plasmon resonance and fluorescence microscopy is described. The host shows selectivity for choline-derived substrates, and no competitive incorporation of substrate is observed in the membrane bilayer. A variety of trimethylammonium-derived substrates are suitable guests, displaying binding affinities in a millimolar range. The membrane:cavitand:guest complexes can be subsequently used to capture NeutrAvidin protein at the membrane surface if a biotin-derived guest molecule is used. The surface coverage of NeutrAvidin is affected by the spacer used to derivatize the biotin. Increased distance from the bilayer allows a higher concentration of protein to be immobilized, suggesting a diminishing detrimental steric effect when the binding event is shifted away from the surface.

Introduction

The surfaces of mammalian cells are decorated with a wide variety of membrane-bound receptor molecules. These receptors act as sensors for, and transporters of small molecules in the extracellular environment.1 For example, acetyl-cholinesterase is a membrane-bound protein that binds the target acetylcholine via non-covalent cation-π interactions with active site aromatic residues.2 These natural receptors have inspired the discovery of new methods to transport polar drug candidates across hydrophobic membrane bilayers, a process of great importance to medicinal chemistry. 3 Small molecules have been exploited to induce endocytosis 4 or to hydrophobically shield the drug candidate as it is transported through the membrane.5 Many examples of targeted drug delivery use natural receptors such as glycolipids6 or polypeptides4b to recognize the target, or study the transport process alone by covalently linking the drug target to a suitable vector.5 In these cases, the artificial membrane receptors typically consist of the covalent attachment of the recognition motif to a lipid or steroid derivative that is incorporated in a synthetic membrane. The recognition motif is displayed above the membrane surface in order to bind to the target.

An alternate method of substrate recognition is the incorporation of a defined binding pocket *inside* the membrane bilayer. This strategy is employed by membrane-penetrating proteins7 and transmembrane pore-forming peptides8 – the host is incorporated in the membrane itself, and displays a cavity that allows polar substrates to be shielded from the lipophilic

richard.hooley@ucr.edu; quan.cheng@ucr.edu.

Supporting Information Available: SPR sensorgrams and binding calculations. This material is available free of charge via the internet at http://pubs.acs.org.

NIH-PA Author Manuscript
NIH-PA Author Manuscript
NIH-PA Author Manuscript

NIH-PA Author Manuscript

NIH-PA Author Manuscript

NIH-PA Author Manuscript

membrane.9 This is mainly exploited for substrate transport *through* the membrane, but a synthetic host that displayed this type of binding motif would show a far greater range of application than receptors created *via* the covalent derivatization of steroids and lipids. To achieve this, we require a synthetic cavity that can be incorporated into a membrane bilayer while still retaining selective host properties. Most water-soluble synthetic host molecules take advantage of the hydrophobic effect to recognize their desired targets,10 which poses a problem for application in natural systems. Hydrophobic substrates suffer from poor water-solubility and non-specific localization in the lipophilic membrane bilayers present in cells. In addition, competitive binding of hydrophobic lipids themselves inside the host will reduce the affinity for the target substrate. Because of these factors, the use of cavity-based synthetic receptors in natural systems is underexplored.

Deep cavitands11 are well-known as protein mimics, in that they provide a cavity that can selectively recognize molecules of the correct shape if they also contain a thin layer of positive charge at their surface. 12 Excellent selectivity for substituted trimethylammonium salts is possible in both water13 and organic solvents.14 Recognition of hydrocarbons15 and steroids16 *via* the hydrophobic effect has also been reported. As well as binding hydrophobic species, molecules such as Rebek's tetracarboxylate cavitand **1** (Figure 1) have shown the ability to be incorporated in lipid micelles.17 The host:guest properties of these small micellar aggregates were studied by 1D NMR and diffusion NMR techniques, indicating that the molecules were able to bind suitable guests in the presence of lipids above the critical micelle concentration, albeit with reduced affinities with respect to those in pure water. Analysis of the composition of the micelles was not performed, nor were studies carried out on larger aggregates such as vesicles or membrane bilayers. In order to apply this proof of principle to more biorelevant settings, analysis of the host properties in bilayers and vesicles is required. NMR analysis of the micellar properties provides some information, but ^{1}H NMR spectroscopy is poorly suited for analysis of membrane bilayers due to the substantial signal broadening observed. A different sensing technique is therefore required.

Supported lipid bilayers are an excellent mimic of natural membranes, as they maintain similar fluidity properties18 and substrate mobility. These membrane mimics have been successfully used for the study of a variety of biological phenomena.19 The predominant technique for characterizing activities on the membrane has been fluorescence microscopy, while in recent years label-free methods such as surface plasmon resonance have gained considerable application due to simple experimental procedure and real-time measurement capability.20 Proper functionalization of the gold substrates by hydrophilic polymers in SPR is required in order to fabricate quality membrane mimics. Recently an improved approach using a calcinated nanoglassified gold surface has come forward and allowed direct assembly of the supported membranes at the sensing interface,21 allowing the real-time detection of binding events in a supported membrane bilayer. The binding properties of proteins such as lectins22 and bacterial toxins23 have been extensively assessed with the calcinated gold chips.

Synthetic host molecules, such as calixarenes, shallow cavitands and cyclodextrins, have been directly attached to surfaces for sensing applications.24 They have been tested for detection of a range of small molecules including gas vapors, polycyclic aromatic hydrocarbons via surface-enhanced Raman spectroscopy (SERS),25 and adrenaline/catecholamine via electrochemistry.26 The results show satisfactory sensitivity, however detection of small molecules by SPR can be challenging to implement as low molecular weight compounds are insufficiently large to generate a measurable refractive index change. SPR sensing of small molecule interactions in a supported bilayer poses an even greater challenge, as the recognition event is displaced from the surface. In addition, the binding

NIH-PA Author Manuscript

NIH-PA Author Manuscript

NIH-PA Author Manuscript

constants obtainable by synthetic receptors are generally on the order of millimolar (with some notable exceptions27), rather than the micro- and nanomolar binding affinities displayed by proteins. Binding properties of lectins that show millimolar binding affinities are detectable,28 but any receptor incorporated in the membrane must display at least millimolar affinity for substrate in order for accurate analysis to be possible.

In this work, small molecule interactions with cavitand incorporated supported bilayer lipid membrane are investigated by SPR spectroscopy. The use of calcinated surface offers an enhanced mode of SPR detection, allowing study of the interactions of cavitands such as **1** with a series of choline derivatives in a near-native cell membrane mimic. The binding events are exploited to understand the interactions between polar guests and the water-soluble host in biomimetic media, while the employment of biotin-tagged guests aims to further explore the protein binding properties at the membrane surface via a host:guest handle.

Experimental

^{1}H spectra were recorded on a Varian Inova 400 spectrometer. Proton (^{1}H) chemical shifts are reported in parts per million (δ) with respect to tetramethylsilane (TMS, δ = 0), and referenced internally with respect to the protio solvent impurity. Deuterated NMR solvents were obtained from Cambridge Isotope Laboratories, Inc., Andover, MA, and used without further purification. 1-Palmitoyl-2-oleoyl-sn-glycero-3-phosphocholine was purchased from Avanti Polar Lipids. All other materials were obtained from Aldrich Chemical Company, St. Louis, MO and were used as received. Solvents were dried through a commercial solvent purification system (SG Water, Inc.). Cavitands **1-3** were synthesized according to literature procedures.13b,14

2-Thioureidonaphthalene-ethyltrimethylammonium chloride 5

2-Naphthyl isothiocyanate (19 mg, 0.10 mmol) was added to a solution of 2-aminoethyl-trimethylammonium chloride (18 mg, 0.10 mmol) and Et_3N (10 μL) in DMSO (0.6 mL). After stirring for 1 hr at 70 °C, the solution was added to acetone (5 mL) and hexane (5 mL). The oily residue was separated by centrifugation, then added to 10% aqueous NaOH solution (1.5 mL) and washed with ethyl acetate (5 mL × 2). After neutralizing with 10% HCl solution, the solvent was removed *in vacuo* to furnish product **5** (15 mg, 46%). ^{1}H NMR (400 MHz, DMSO-d_6) δ 11.93 (s, 1H), 10.40 (s, 1H), 8.20 (s, 2H), 7.80 (dd, J = 8.6 Hz, 17.7, 7H), 7.69 (dd, J = 2.1 Hz, 8.8, 2H), 7.42 (dt, J = 7.5 Hz, 15.9 Hz, 4H), 3.56 (t, J = 6.3 Hz, 4H), 3.31 (t, J = 6.9 Hz, 4H), 3.17 (s, 9H); ^{13}C NMR (100 MHz, DMSO-d_6) δ 182.27, 139.00, 134.09, 131.32, 128.47, 128.17, 127.11, 125.66, 124.32, 119.38, 105.16, 64.80, 53.68, 38.52. HRMS (ESI) m/z: calcd for $C_{16}H_{22}N_3S$ (M^+) 288.1529; found 288.1537.

2-(Thioureidofluorescein)-ethyltrimethylammonium chloride 6

Fluorescein isothiocyanate (39 mg, 0.10 mmol) was added to a solution of 2-aminoethyl-trimethylammonium chloride (17 mg, 0.10 mmol) and K_2CO_3 (28 mg, 0.20 mmol) in water (1.5 mL). After stirring for 18 hr at room temperature, the solution was filtered and the filtrand was added to acetone (5 mL). The precipitate was separated by centrifugation and washed with acetone (3 mL) twice providing the desired compound **6** as a red solid (18 mg, 34%). ^{1}H NMR (400 MHz, D_2O) δ 7.70 (d, J = 2.1 Hz, 1H), 7.50 (dd, J = 2.2 Hz, 8.2 Hz, 1H), 7.21 (m, 3H), 6.68–6.60 (m, 4H), 4.13 (t, J = 6.6 Hz, 2H), 3.63 (t, J = 6.8 Hz, 2H), 3.25 (s, 10H); ^{13}C NMR (100 MHz, D_2O) δ 180.79, 174.09, 157.75, 148.99, 143.98, 141.19, 131.49, 130.03, 126.16, 124.86, 123.02, 112.52, 103.77, 63.91, 53.54, 38.73; HRMS (ESI) m/z: calcd for $C_{26}H_{26}N_3O_5S$ (M^+) 492.1588; found 492.1587.

NIH-PA Author Manuscript

NIH-PA Author Manuscript

NIH-PA Author Manuscript

2-Biotinamidyl-ethyltrimethylammonium chloride 7

Isobutyl chloroformate (16 μL) was added to a solution of biotin (25 mg) in DMF (0.6 mL) containing tri-N-butylamine (32 μL). After 10 min at room temperature, the mixture was added to a solution of 2-aminoethyl-trimethylammonium chloride (18 mg, 0.10 mmol) in DMF/water (1:1). After stirring at room temperature overnight, added to 10% NaOH solution (1.5 mL) and washed with ethyl acetate (5 mL × 2). After neutralizing with 10% HCl solution, the solvent was removed *in vacuo* to furnish product **7** (18 mg, 49%).

^{1}H NMR (400 MHz, D_2O) δ 4.66 (dd, *J* = 4.7 Hz, 7.8, 1H), 4.47 (dd, *J* = 4.5 Hz, 7.9, 1H), 3.74 (t, *J* = 6.3 Hz, 2H), 3.54 (t, *J* = 6.7 Hz, 2H), 3.44–3.34 (m, 1H), 3.23 (s, 9H), 3.05 (q, *J* = 5.1 Hz 1H), 2.83 (d, *J* = 13.1 Hz, 1H), 2.35 (t, *J* = 7.3 Hz, 2H), 1.84–1.56 (m, 4H), 1.52–1.38 (m, 2H); ^{13}C NMR (100 MHz, D_2O) δ 177.54, 165.52, 64.34, 62.26, 60.42, 55.52, 53.50, 39.84, 35.41, 33.59, 28.07, 27.81, 24.97. HRMS (ESI) m/z: calcd for $C_{15}H_{29}N_4O_2S$ (M^+) 329.2006; found 329.2007.

2-Biotinamidyl-caproylethyltrimethylammonium chloride 8

Isobutyl chloroformate (9 μL) was added to a solution of biotinylaminohexanoic acid29 (18 mg) in DMF (0.6 mL) containing tri-N-butylamine (30 μL). After 10min at room temperature, the mixture was added to a solution of 2-aminoethyl-trimethylammonium chloride (9 mg, 0.05 mmol) in DMF/water (1:1). After stirring at room temperature overnight, added to 10% NaOH solution (1.5 mL) and washed with ethyl acetate (5 mL × 2). After neutralizing with 10% HCl solution, the solvent was removed *in vacuo* to furnish product **8** (20 mg, 83%). ^{1}H NMR (400 MHz, D_2O) δ 4.64 (dd, J = 5.0, 8.0, 1H), 4.46 (dd, J = 4.5, 7.9, 1H), 3.72 (t, J = 6.7, 2H), 3.51 (t, J = 6.7, 2H), 3.44–3.33 (m, 1H), 3.21 (s, 9H), 3.03 (q, J = 5.0 Hz, 1H), 2.82 (d, *J* = 13.1 Hz, 1H), 2.35–2.24 (m, 4H), 1.82–1.50 (m, 8H), 1.48–1.40 (m, 2H), 1.39–1.30 (m, 2H). ^{13}C NMR (100 MHz, D_2O) δ 177.52, 176.79, 165.50, 64.32, 62.24, 60.41, 55.52, 53.50, 39.87, 39.19, 35.63, 33.60, 28.16, 27.98, 27.83, 25.76, 25.35, 24.88, 23.37. HRMS (ESI) m/z: calcd for $C_{21}H_{40}N_5O_3S$ (M^+) 442.2846; found 442.2845.

Calcinated chip preparation—Gold substrates were fabricated with a 2 nm thick chromium adhesion layer, followed by deposition of a 46 nm thick gold layer *via* e-beam evaporation onto cleaned glass slides. The nanoglassified layers were constructed on the surface based on a previous layer-by-layer protocol.30 Clean gold substrates were immersed in 10 mM 3-mercaptopropionic acid (MPA) ethanol solution overnight to form a self-assembled monolayer. After extensive rinsing with ethanol and nanopure water and drying with nitrogen gas, modified gold substrates were alternated dipped into sodium silicate solution (22 mg/mL, adjusted to pH 9.5) and poly(allylamine hydrochloride) solution (1 mg/mL, adjusted to pH 8.0) for 1 min to form a layer by layer assembly structure, with sufficient nanopure water rinsing between layers. This dipping process was repeated eight times to build up a multilayered chip, followed by calcination in a furnace by heating to 450 °C at a rate of 17 °C per min and subsequent cooling to room temperature 4 hours later.

Vesicle preparation—PC lipid stock solution was transferred to a small vial and the organic solvent was purged from the vial with N_2 to form a dry lipid film on the vial wall, which was then rehydrated with 20 mM phosphate buffered saline (150 mM NaCl, pH 7.40) to a lipid concentration of 1 mg/mL. The resuspended lipids were probe sonicated for 20 min, followed by centrifugation at 8000 rpm for 6 min to remove any titanium particles released from the probe tip. The supernatant was then extruded with 11 passes through a polycarbonate membrane of pore size 100 nm to ensure formation of small unilamellar vesicles. The solution was then incubated at 4 °C for at least 1 h before use.

NIH-PA Author Manuscript

NIH-PA Author Manuscript

NIH-PA Author Manuscript

Fabrication of cavitand 1 receptor layer and guest binding measurement—The fabrication of cavitand **1** - membrane complex and subsequent guest binding was monitored through surface plasmon resonance (SPR) spectrometry and fluorescence microscopy. The shift of SPR minimum angle characterized surface thickness and surface refractive index change, demonstrating adsorption or binding on the surface. The calcinated gold substrate was first rinsed with ethanol and nanopure water and after drying under a gentle stream of N_2 gas, then was clamped down by a flow cell on a high-refractive index prism for SPR measurement. 1 mg/mL PC vesicles in 20mM phosphate buffered saline (150 mM NaCl, pH 7.40) were injected through a flow-injection system, and incubated for 1 h to allow vesicle fusion on the hydrophilic calcinated gold surface, forming a smooth bilayer membrane. After 10 min rinsing to remove excess vesicle from the surface, 2 mg/mL cavitand **1** in 10% DMSO solution was subsequently injected and incubated for 20 min. The surface was extensively rinsed with nanopure water, followed by incubation with 2 mM aqueous solution of guest **4**–**8** for varied times. Control experiments were performed under identical conditions in the absence of cavitand **1**.

For fluorescein guest **6**, fluorescence microscopy experiments were also performed on the same chip setup. After sufficient rinsing with nanopure water, fluorescence microscopy was carried out on a Zeiss LSM 510 confocal laser scanning microscope with 488 nm argon laser excitation and a CCD camera. For comparison, an aqueous solution of guest **6** was injected onto the PC membrane surface as before, in the absence of cavitand **1**.

Surface coverage calculations

The surface coverage of adsorbates on a membrane bilayer can be estimated via Jung's formula (eq 1) when the membrane between adsorbate and metal surface is very thin compared to plasmon decay length.31 Cavitand **1** surface coverage (in units of molecules/cm^2) can be estimated by the SPR signal increase:

$$\theta = \mathrm{N} I_d / 2[\mathrm{R}/m(\eta_a - \eta_s)] \quad (1)$$

where N is the bulk number density of the adsorbate; I_d is roughly estimated as 0.37 of the light wavelength (670 nm here); R is SPR response (in the unit of degrees) via binding; *m* is a instrument constant (determined experimentally by calibrating the measured sensor response to changes in refractive index); η_a is the refractive index of adsorbed molecule and η_s is the refractive index of bulk solution (1.33 for water). I_d is much larger than the thickness of bilayer lipid membrane (~5 nm), allowing correct application of equation (1).31

To calculate the surface coverage of cavitand **1**, the bulk refractive index of cavitand **1** was estimated as 1.6013 and bulk density was estimated as 1.1254 g/cm^3.32 From SPR signal increase upon cavitand **1** binding (0.20 ± 0.02 degree), θ was determined to be 8.02 ± 0.93 × 10^{13} molecules/cm^2. NeutrAvidin binding to the **1**·**7** complex caused a signal increase of 0.25 ± 0.05 degree. Crystalline protein refractive index (1.60) was used as bulk refractive index,31 and 1.43 g/cm^3 as bulk density,33 thus θ of NeutrAvidin was determined to be 2.94 ± 0.62 × 10^{12} molecules/cm^2.

Kinetic analysis

Saturation binding mode (eq 2)23 was applied here to determine the equilibrium dissociation constant (K_D) value for the interaction between cavitand **1** and guest **6**. Increasing concentrations of guest **6** (0.5 mM to 5 mM) were injected over the cavitand **1**:membrane complex, and the minimum angle shift was recorded:

NIH-PA Author Manuscript

NIH-PA Author Manuscript

NIH-PA Author Manuscript

$$AB_{eq}=AB_{max}(1/(1+K_D/[A])) \quad (2)$$

where AB_{eq} is the average of response signal at equilibrium and AB_{max} is the maximum response that can be obtained for guest **6** binding and [A] is the concentration of guest **6** injection. AB_{max}/AB_{eq} was plotted against 1/[A], and the slope is equal to K_D value (3.54 ± 0.92 mM). K_A, the equilibrium association constant (282 ± 73 M^{-1}), can be determined by the reciprocal value of K_D. This process was used to determine K_D/K_A for guests **6, 7, 8** and NeutrAvidin.

In transient SPR response mode,34 the initial rate kinetic method was employed to extract association constant (k_{assoc}), dissociation constant (k_{diss}), and K_D value for the interaction between cavitand **1** and guest **6**. At t = 0, the equation for initial rate analysis is

$$dAB/dt=AB_{max}[A]k_{assoc} \quad (3)$$

By plotting the initial rate against [A], k_{assoc} was calculated as 289.76 M^{-1} min^{-1}. k_{diss} can be determined from the dissociation curve of SPR sensorgram:

$$AB_t=(AB_0 - AB_\infty)[\exp(-k_{diss}t)]+AB_\infty \quad (4)$$

where AB_0 is the initial response at the beginning of the dissociation curve, AB_∞ is the final response once completely dissociated. Given k_{diss} value is 1.304 min^{-1}, K_D is thus determined to be 3.54 mM via $K_D = k_{diss}/k_{assoc}$.

Results and Discussion

Three cavitands were initially tested for their associative properties with the membrane bilayer; water-soluble tetracarboxylate cavitand **1**, and its more lipophilic counterparts **2** and **3**. The synthesis of **1-3** and their binding properties in both water and organic solvents have been previously reported.13،14، 35 Cavitand **1** is soluble in water at millimolar concentrations, whereas lipophilic cavitands **2** and **3** are only sparingly soluble in pure water, but can be incorporated into micelles in the presence of added lipid.17b All three hosts show millimolar affinity for choline and related trimethylammonium salts due to favorable cation-π interactions between the aromatic cavitand walls and the guest. In water, choline has a binding affinity for **1** of 2.6 × 10^4 M^{-1}, although the K_A was lessened in an SDS micelle.17a A significant advantage of cavitands as hosts is their open-ended character; long guests can extend out of the cavity, presenting large functional groups into the bulk solvent. This allows a variety of guest derivatives to be tested.

The experiment is illustrated in Scheme 1. The membrane was deposited on a nanoglassified gold chip in a flow-cell (see Experimental).22 The membrane was fabricated by the injection of preformed L-α phosphatidylcholine (PC) vesicles that fuse readily on this chip. Cavitands **1-3** were subsequently injected into the system in a 10% DMSO:H_2O solution (to maximize solubility) followed by a rinsing stage to remove all DMSO and unincorporated cavitand from the flowcell. Finally, a suitable guest (Figure 1c) was introduced to the system by injection, followed by copious rinsing to remove the unincorporated excess. PC was chosen as the constituent lipid to minimize the host:guest binding of the lipid inside the cavitand. The two alkyl chains in PC (oleoyl and palmitoyl) cannot both fit inside the cavity (as has been observed with SDS17a), and the phosphate anion in the phosphocholine group

NIH-PA Author Manuscript

NIH-PA Author Manuscript

NIH-PA Author Manuscript

minimizes binding at that terminus *via* a repulsive interaction with the carboxylates at the cavitand rim.13b

The effect of addition of cavitand **1** to the membrane bilayer is shown by the SPR sensorgram in Figure 2. The change in resonance angle upon addition indicates the binding of cavitand **1** to the PC membrane. The cavitand remains bound to the membrane bilayer even after extensive rinsing, and the angular shift indicates a surface coverage of $8.02 \pm 0.93 \times 10^{13}$ molecules/cm^2 (see Experimental). The incorporation of cavitands **2** and **3** in the PC membrane was also observed, but with a substantially lower change in SPR signal and thus, surface coverage. We attribute this to their poor solubility in water and limited exposure to the membrane in the flowcell setting. All subsequent analyses were performed using water-soluble cavitand **1**.

The sensorgram does not, however, give any indication of the orientation of cavitand **1** in the membrane. To determine whether its binding properties remained intact, the cavitand:membrane system was exposed to the guest molecules shown in Figure 1c. To minimize nonspecific interaction between the guest and the membrane bilayer, commercially available long chain alkyltrimethylammonium salts were avoided. The guests used in this study were synthesized by the coupling of 2-(trimethylammonium)ethylamine chloride with either the isothiocyanate (**5,6**) or acid chloride (**7,8**) of the corresponding headgroup (Figure 1c). All showed good water solubility (≥ 20 mM), and were analyzed by ^{1}H NMR spectroscopy before injection.

Upon addition of choline **4**, no change in resonance angle was observed. This is not entirely unexpected, as molecular modeling (Figure 1b) indicates that choline is completely surrounded by the cavity upon binding, and does not protrude into the solvent above the membrane. The small change in the membrane composition upon small guest binding would be difficult to detect, however, so host:guest affinity cannot be ruled out. Upon addition of larger guests **5–8** to the system, a small, reproducible change in resonance angle was observed, indicating guest binding and concomitant change in refractive index of the membrane. The SPR response to guest binding was dependent on the molecular weight of the substrate. SPR signal response increased with increasing guest molecular weight, and corresponding increase in perturbation of the environment at the membrane-water interface. The change in resonance angle for the three largest guests **6-8** was large enough to allow reasonably accurate calculation of K_D/K_A values, although this was not possible for smaller guests **4** and **5**.

The values of equilibrium dissociation constant (K_D) and binding affinity (K_A) for the host:guest interactions between guests **6-8** and cavitand **1** were determined from SPR sensorgrams via saturation binding mode (see Experimental section). Guest **6** showed millimolar binding affinity ($K_D = 3.54 \pm 0.92$ mM, $K_A = 282 \pm 73$ M^{-1}). This value is two orders of magnitude smaller than that observed for substituted trimethylammonium salts in pure water, but is consistent with the binding affinity observed under physiological conditions (phosphate buffer, as used in these experiments).13b For comparison, the transient SPR response method was also used to determine the binding constant to the cavitand:membrane complex. The K_D value (4.55 mM) agrees well with the number derived from equilibrium binding analysis. A stronger affinity was determined for biotin-derived guests **7** (K_D (**7**·**1**) = 1.87 ± 0.24 mM, $K_A = 535 \pm 68$ M^{-1}) and (**8** K_D (**8**·**1**) = 1.95 ± 0.61 mM, $K_A = 513 \pm 160$ M^{-1}). These binding affinities show that the cavitand retains most of its host abilities while incorporated in the membrane. Furthermore, control experiments in the absence of cavitand **1** show no SPR response from addition of any of the guests **4-8** to the supported membrane. This indicates that there is no non-specific incorporation of the targets in the membrane even in the case of mildly lipophilic naphthalene guest **5**.

NIH-PA Author Manuscript

NIH-PA Author Manuscript

NIH-PA Author Manuscript

It should be noted that although the changes in resonance angle observed upon guest binding are small, the measurements are reproducible. Further evidence for guest incorporation was obtained by fluorescence microscopy. Construction of the membrane:cavitand **1**:guest **6** complex was performed as before, and the chip visualized under a confocal microscope. The fluorescence microscopic images are shown in Figure 3. After extensive rinsing, the boundary of the flow cell with **6** was clearly visible, demonstrating fluorescence signal from the guest **6**·cavitand **1** complex incorporated in the membrane bilayer. The host:guest system was strong enough to retain the substrate in the membrane for a period of many minutes under rinse conditions. In the absence of cavitand, little fluorescence was observed under the same excitation condition, providing further evidence that there was little nonspecific adsorption of **6** on the membrane.

The result also illustrates the advantage of the choline-based guest system. Non-specific interaction between organic molecules and membrane bilayers is a significant problem when creating shape-based receptors for membranes. Hydrophobic substrates would be susceptible to incorporation in the membrane itself, but that is not observed in this case; negligible binding of the guests **4**-**8** can be observed in the absence of cavitand by either fluorescence (if applicable) or SPR.

These results show that cavitand **1** is able to non-covalently bind a variety of trimethylammonium-tagged species while incorporated in the supported membrane bilayer. The open-ended nature of the cavitand allows a wide scope of guest size; the trimethylammonium group is bound in the cavity, and the unencapsulated portion of the guest is displayed above the membrane surface. This suggests that a guest that contains a recognition element *itself* should be able to recognize its target while bound to the membrane:cavitand complex. Compounds **7** and **8** were used for this purpose. Both guests display a biotin group above the membrane surface, differing only in the space between the biotin recognition motif and cavitand/membrane complex.

Upon addition of NeutrAvidin to the preformed membrane:cavitand **1**:guest **7** complex, a significant change in resonance angle ($\Delta R = 0.20 \pm 0.02$ deg) was observed, indicating that the complex is capable of displaying the biotin tag above the membrane while retaining its affinity for a suitable protein. As would be expected due to its much greater size and charge, NeutrAvidin displays a significantly larger ΔR upon binding than observed for the binding of guests **5**–**8**. Both biotin-derived guests **7** and **8** displayed affinity for NeutrAvidin (the SPR sensorgrams for guest **7** are shown in Figure 4, and those for guest **8** are shown in the Supporting Information). The sequential binding of cavitand, guest and NeutrAvidin are all observable. Addition of NeutrAvidin to the membrane:cavitand **1**: guest **8** complex caused a much larger change in resonance angle ($\Delta R = 0.42 \pm 0.06$ deg).

Control experiments were performed by substituting biotin itself for guests **7**/**8** (Figure 4b), and the addition of guests **7**/**8** to the membrane followed by NeutrAvidin in the absence of cavitand **1**. All controls were performed with the same concentration of guests. The sensorgram in Figure 4b displays no increase in resonance angle upon addition of biotin or NeutrAvidin, indicating minimal nonspecific interactions of the protein or biotin with the cavitand or the membrane itself. In the absence of cavitand **1**, (Figure 4c), neither guest **7** nor NeutrAvidin show significant incorporation in the membrane. Presence of both cavitand **1** and the trimethylammonium binding handle are required to attach the protein to the surface; a four-component binding event is seen, with only non-covalent interactions binding the cavitand, guest and NeutrAvidin to the supported membrane bilayer. The binding affinities are strong enough to hold the four-component complex together during the final washing phase.

NIH-PA Author Manuscript

NIH-PA Author Manuscript

NIH-PA Author Manuscript

The NeutrAvidin surface coverage was calculated by SPR response as before. When immobilized by the cavitand **1**·guest **7** complex, NeutrAvidin surface coverage was estimated to be $2.94 \pm 0.62 \times 10^{12}$ molecules/cm^2, (c.f. θ (cavitand **1**) = $8.02 \pm 0.93 \times 10^{13}$ molecules/cm^2). The cavitand:NeutrAvidin ratio is 27.3: 1, which is to be expected due to the vast difference in sizes between cavitand **1** (MW = 1377 Da) and NeutrAvidin (MW = 60 kDa). The millimolar binding affinity of guest **7** will also contribute to this difference, as not all host molecules will be occupied.

Although there was minimal change in the binding affinity for guests **7** and **8** in cavitand **1**, a significant difference in SPR response was detected upon NeutrAvidin binding. The surface coverage of NeutrAvidin when bound to the PC·**1**·guest **8** complex is $4.94 \pm 0.71 \times 10^{12}$ molecules/cm^2, which is two-fold greater than that observed for the shorter guest **7**. This is most likely due to reduced steric interactions between the protein and the membrane bilayer when the longer guest **8** is used as the recognition motif.

In addition to the surface coverage experiments, the binding affinity of NeutrAvidin for the cavitand·guest complex could be measured. This is unusual as the biotin:NeutrAvidin binding affinity is ~10^{15} M^{-1}, far too high for analysis by SPR. In this case, the saturation binding mode gave the biotin:NeutrAvidin binding constant of 3.64×10^5 M^{-1}. This lowered binding affinity is most likely not due to the biotin:NeutrAvidin interaction, but the interaction between NeutrAvidin·**8** complex and the membrane:cavitand complex – the "weakest link" is the cavitand:trimethylammonium interaction, and some of the guest may be pulled out of the cavitand upon NeutrAvidin coordination. Given that the binding affinity is at least partially driven by the hydrophobic effect,36 it is unsurprising that the affinity decreases upon conversion of the small **8** to the large, extremely hydrophilic NeutrAvidin·**8** complex. The binding affinity was determined by regression analysis, and the best fit was obtained by assuming a 1:1 biotin:avidin binding motif. It is possible that multivalent binding between NeutrAvidin and the **1**·**8** complex can occur,37 but our binding data suggests this is not dominant in this case, most probably due to the low density of **1**·**8** in the membrane.

Figure 5 shows an illustration of the relative sizes of the cavitand, guest and lipid bilayer (as determined by molecular modeling; SPARTAN, AM1 forcefield). The cavitand is relatively small, with a vertical height of approximately 13 Å. When compared to the POPC length (~26 Å), it becomes clear that the cavitand is most likely positioned towards the top of the lipid bilayer, incorporated in the first layer such that the negatively charged carboxylates are in proximity with the aqueous exterior, and the hydrophobic cavitand body is incorporated amongst the lipid hydrocarbon chains. This allows the host to present suitable guests to the exterior milieu.

The binding abilities of the membrane:cavitand:trimethylammonium complexes are quite remarkable – in the presence of lipids that can act as competitive substrates, in buffered solution that lowers substrate affinity and shear forces from the flowcell, a host the diameter of only *two* POPC lipid molecules is able to immobilize a 60 KDa protein. This protein is held in place solely by cation-π interactions between eight aromatic rings and a single trimethylammonium cation. Cation-π interactions are a vital component of protein:substrate recognition events,38 but this shows their potential as the "mortar" holding together quaternary nanoscale constructs.

Conclusions

In this work, we have shown that a deep water-soluble cavitand can be incorporated in a membrane bilayer attached to a nanoglassified surface, while still retaining its host

NIH-PA Author Manuscript

NIH-PA Author Manuscript

NIH-PA Author Manuscript

properties. The open-ended nature of the cavitand allows binding of a variety of guest sizes; the trimethylammonium binding "handle" is incorporated inside the cavity while the rest of the molecule is displayed above the cavity in the aqueous phase. Competitive binding from the membrane lipids is minimal, and association constants on the order of 10^3 M^{-1} are observed with a variety of trimethylammonium-derived substrates. The binding events can be observed in real-time by SPR spectroscopy, and the binding of fluorescent derivatives observed by fluorescence microscopy. No non-specific binding of the guest molecules in the membrane itself can be observed in the absence of cavitand – the host can selectively recognize its targets in a biorelevant setting. The membrane:cavitand:guest complexes can subsequently be used to sense proteins at the membrane surface. By the use of a suitable biotin-derived guest molecule, the biotin motif is displayed above the membrane bilayer, and is able to immobilize NeutrAvidin at the surface, a process detectable by SPR. The surface coverage is dependent on the spacer used to derivatize the biotin – increased distance from the bilayer allows a higher concentration of protein to be immobilized.

These binding studies showcase the potential of this system as a host for larger, more hydrophilic aggregates – the trimethylammonium:cavitand interaction is not just a product of the hydrophobic effect, so is tolerant to the binding of highly hydrophilic species such as proteins. Lipid/steroid "anchors" can be rendered useless if the external group is too hydrophilic (as has been observed for lipophilic oligonucleotides39); exploiting non-hydrophobic interactions to anchor species in a membrane can allow a far greater range of target species. Further studies on the properties of membrane-bound hosts are underway.

Supplementary Material

Refer to Web version on PubMed Central for supplementary material.

Acknowledgments

We are grateful to Profs. Julius Rebek, Jr. and Michael Schramm for helpful discussions. QC acknowledges financial support from NSF (CHE-0719224).

References

1. Conner SD, Schmid SL. Nature. 2003; 422:37–44. [PubMed: 12621426]
2. Sussman JL, Harel M, Frolow F, Oefner C, Goldman A, Toker L, Silman I. Science. 1991; 253:872–879. [PubMed: 1678899]
3. a) Langer R. Science. 1990; 249:1527–33. [PubMed: 2218494] b) Langer R. Acc Chem Res. 1993; 26:537–542. c) Peterson BR. Org Biomol Chem. 2005; 3:3607–3612. [PubMed: 16211095]
4. a) Boonyarattanakalin S, Martin SE, Dykstra SA, Peterson BR. J Am Chem Soc. 2004; 126:16379–16386. [PubMed: 15600339] b) Boonyarattanakalin S, Hu J, Dykstra-Rummel SA, August A, Peterson BR. J Am Chem Soc. 2007; 129:268–269. [PubMed: 17212394] c) Boonyarattanakalin S, Martin SE, Sun Q, Peterson BR. J Am Chem Soc. 2006; 128:11463–11470. [PubMed: 16939269]
5. a) Janout V, Lanier M, Regen SL. J Am Chem Soc. 1996; 118:1573–1574. b) Janout V, Lanier M, Regen SL. J Am Chem Soc. 1997; 119:640–647. c) Janout V, DiGiorgio C, Regen SL. J Am Chem Soc. 2000; 122:2671–2672. d) Kondo M, Mehiri M, Regen SL. J Am Chem Soc. 2008; 130:13771–13777. [PubMed: 18783220] d) Mehiri M, Chen WH, Janout V, Regen SL. J Am Chem Soc. 2009; 131:1338–1339. [PubMed: 19140686]
6. Bertozzi CR, Kiessling LL. Science. 2001; 291:2357–2364. [PubMed: 11269316]
7. Mackenzie KR. Chem Rev. 2006; 106:1931–1977. [PubMed: 16683762]
8. a) Ghadiri MR, Granja JR, Buehler LK. Nature. 1994; 369:301–304. [PubMed: 7514275] b) Granja JR, Ghadiri MR. J Am Chem Soc. 1994; 116:10785–10786. c) Thorén PEG, Persson D, Esbjörner EK, Goksör M, Lincoln P, Nordén B. Biochemistry. 2004; 43:3471–3489. [PubMed: 15035618]
9. Cho W, Stahelin RV. Annu Rev Biophys Biomol Struct. 2005; 34:119–151. [PubMed: 15869386]

NIH-PA Author Manuscript NIH-PA Author Manuscript NIH-PA Author Manuscript

10. Biros SM, Rebek J Jr. Chem Soc Rev. 2007; 36:93–105. [PubMed: 17173148]
11. Rudkevich DM, Hilmersson G, Rebek J Jr. J Am Chem Soc. 1998; 120:12216–12225.
12. Hooley RJ, Rebek J Jr. Chem Biol. 2009; 16:255–264. [PubMed: 19318207]
13. a) Hof F, Trembleau L, Ullrich EC, Rebek J Jr. Angew Chem Int Ed. 2003; 42:3150–3153. b) Biros SM, Ullrich EC, Hof F, Trembleau L, Rebek J Jr. J Am Chem Soc. 2004; 126:2870–2876. [PubMed: 14995204]
14. Menozzi E, Onagi H, Rheingold AL, Rebek J Jr. Eur J Org Chem. 2005:3633–3636.
15. a) Hooley RJ, van Anda HJ, Rebek J Jr. J Am Chem Soc. 2007; 129:13464–13473. [PubMed: 17927175] b) Hooley RJ, Biros SM, Rebek J Jr. Chem Commun. 2006:509–510. c) Gibb CLD, Gibb BC. J Am Chem Soc. 2006; 128:16498–16499. [PubMed: 17177388]
16. Gibb CLD, Gibb BC. J Am Chem Soc. 2004; 126:11408–11409. [PubMed: 15366865]
17. a) Trembleau L, Rebek J Jr. Chem Commun. 2004:58–59. b) Schramm MP, Hooley RJ, Rebek J Jr. J Am Chem Soc. 2007; 129:9773–9779. [PubMed: 17636912]
18. Cremer PS, Boxer SGJ. Phys Chem B. 1999; 103:2554–2559.
19. a) Castellana ET, Cremer PS. Surf Sci Rep. 2006; 61:429–444. b) Tanaka M, Sackmann E. Nature. 2005; 437:656–663. [PubMed: 16193040] c) Groves JT, Boxer SG. Acc Chem Res. 2002; 35:149–157. [PubMed: 11900518] d) Schiller SM, Naumann R, Lovejoy K, Kunz H, Knoll W. Angew Chem Int Ed. 2003; 42:208–211. e) Perez JB, Martinez KL, Segura JM, Vogel H. Adv Funct Mater. 2006; 16:306–312.
20. Bieri C, Ernst OP, Heyse S, Hofmann KP, Vogel H. Nat Biotechnol. 1999; 11:1105–1108. [PubMed: 10545918] b) Reimhult E, Larsson C, Kasemo B, Hook F. Anal Chem. 2004; 76:7211–7220. [PubMed: 15595862] c) Wang ZZ, Wilkop T, Cheng Q. Langmuir. 2005; 21:10292–10296. [PubMed: 16262279]
21. a) Phillips KS, Han J, Martinez M, Wang Z, Carter D, Cheng Q. Anal Chem. 2006; 78:596–603. [PubMed: 16408945] b) Han J, Taylor JD, Phillips KS, Wang X, Feng P, Cheng Q. Langmuir. 2008; 24:8127–8133. [PubMed: 18605744] c) Linman MJ, Culver SP, Cheng Q. Langmuir. 2009; 25:3075–3082. [PubMed: 19437774]
22. Linman MJ, Taylor JD, Yu H, Chen X, Cheng Q. Anal Chem. 2008; 80:4007–4013. [PubMed: 18461973]
23. Taylor JD, Linman MJ, Wilkop T, Cheng Q. Anal Chem. 2009; 81:1146–1153. [PubMed: 19178341]
24. a) Daly SM, Grassi M, Shenoy SK, Ugozzoli F, Dalcanale E. J Mater Chem. 2007; 17:1809–1818. b) Schierbaum KD, Weiss T, Thoden van Velzen EU, Engbersen JFJ, Reinhoudt DN, Göpel W. Science. 1994; 265:1413–1415. [PubMed: 17833812] c) Thoden van Velzen EU, Engbersen JFJ, de Lange PJ, Mahy JWG, Reinhoudt DN. J Am Chem Soc. 1995; 117:6853–6862. d) Thoden van Velzen EU, Engbersen JFJ, Reinhoudt DN. J Am Chem Soc. 1994; 116:3597–3598. e) Ludden MJW, Reinhoudt DN, Huskens J. Chem Soc Rev. 2006; 35:1122–1134. [PubMed: 17057841]
25. Guerrini L, Garcia-Ramos JV, Domingo C, Sanchez-Cortes S. Anal Chem. 2009; 81:1418–1425. [PubMed: 19215145]
26. Nikolelis DP, Petropoulou SSE, Theoharis G. Electroanalysis. 2003; 15:1616–1624.
27. Rekharsky MV, Mori T, Yang C, Ko YH, Selvapalam N, Kim H, Sobransingh D, Kaifer AE, Liu S, Isaacs L, Chen W, Moghaddam S, Gilson MK, Kim K, Inoue Y. Proc Natl Acad Sci, USA. 2007; 104:20737–20742. [PubMed: 18093926]
28. Mann DA, Kanai M, Maly DJ, Kiessling LL. J Am Chem Soc. 1998; 120:10575–10582.
29. Skander M, Humbert N, Collot J, Gradinaru J, Klein G, Loosli A, Sauser J, Zocchi A, Gilardoni F, Ward TR. J Am Chem Soc. 2004; 126:14411–14418. [PubMed: 15521760]
30. Linman MJ, Culver SP, Cheng Q. Langmuir. 2009; 25:3075–3082. [PubMed: 19437774]
31. Jung LS, Campbell CT, Chinowsky TM, Mar MN, Yee SS. Langmuir. 1998; 14:5636–5648.
32. Lide, DR., editor. Handbook of chemistry physics. 71. CRC Press; Boston: 1990.
33. Connolly ML. J Mol Graph. 1993; 11:139–141. [PubMed: 8347567]
34. Edwards PR, Leatherbarrow RJ. Anal Biochem. 1997; 246:1–6. [PubMed: 9056175]
35. Far AR, Shivanyuk A, Rebek J Jr. J Am Chem Soc. 2002; 124:2854–2855. [PubMed: 11902859]
36. Hooley RJ, Biros SM, Rebek J Jr. Angew Chem Int Ed. 2006; 45:3517–3519.

NIH-PA Author Manuscript

NIH-PA Author Manuscript

NIH-PA Author Manuscript

37. a) Jung H, Robison AD, Cremer PS. J Struct Biol. 2009; 168:90–94. [PubMed: 19508894] b) Yang T, Baryshnikova OK, Mao H, Holden MA, Cremer PS. J Am Chem Soc. 2003; 125:4779–4784. [PubMed: 12696896] c) Pérez-Luna VH, O'Brien MJ, Opperman KA, Hampton PD, López GP, Klumb LA, Stayton PS. J Am Chem Soc. 1999; 121:6469–6478.

38. Ma JC, Dougherty DA. Chem Rev. 1997; 97:1303–1324. [PubMed: 11851453]

39. a) Bunge A, Kurz A, Windeck AK, Korte T, Flasche W, Liebscher J, Herrmann A, Huster D. Langmuir. 2007; 23:4455–4464. [PubMed: 17367171] b) Jakobsen U, Simonsen AC, Vogel S. J Am Chem Soc. 2008; 130:10462–1046. [PubMed: 18642914]

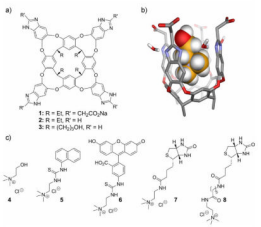

Figure 1.
a) Cavitands **1**-**3**; b) minimized conformation of **1** (SPARTAN, AM1 forcefield) with one bound choline molecule (**4**) in the cavity; c) the guests used in this study.

NIH-PA Author Manuscript
NIH-PA Author Manuscript
NIH-PA Author Manuscript

NIH-PA Author Manuscript

NIH-PA Author Manuscript

NIH-PA Author Manuscript

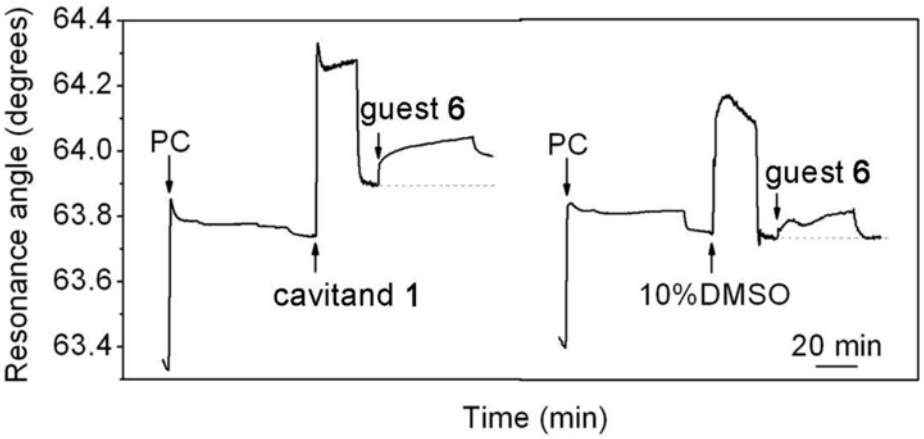

Figure 2.
SPR sensorgrams for guest **6** interaction with PC bilayer membrane in the presence (left) and absence (right) of cavitand **1**.

NIH-PA Author Manuscript

NIH-PA Author Manuscript

NIH-PA Author Manuscript

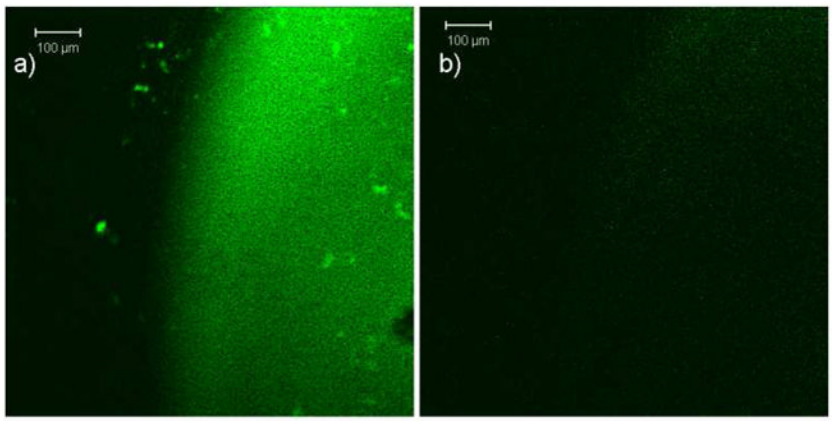

Figure 3.
Fluorescence microscopic images of the calcinated chip containing a) PC bilayer, cavitand **1** and guest **6**; b) PC bilayer and guest **6** alone (control).

NIH-PA Author Manuscript

NIH-PA Author Manuscript

NIH-PA Author Manuscript

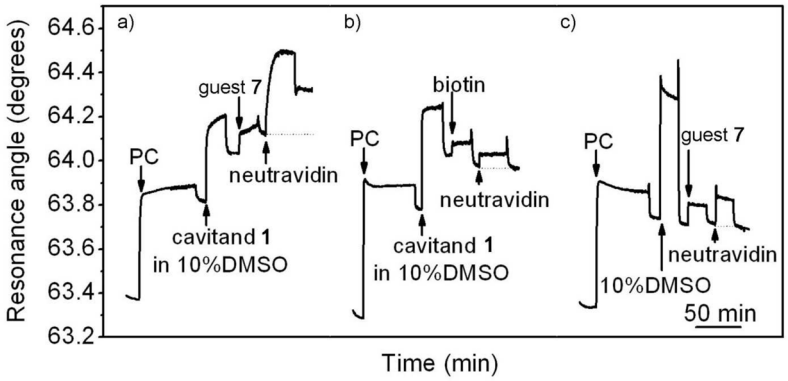

Figure 4.

SPR sensorgrams for NeutrAvidin interaction with a supported PC membrane containing a) cavitand:guest complex **1**·7; b) cavitand **1** and biotin control; c) derivatized biotin guest **7** in the absence of cavitand.

NIH-PA Author Manuscript

NIH-PA Author Manuscript

NIH-PA Author Manuscript

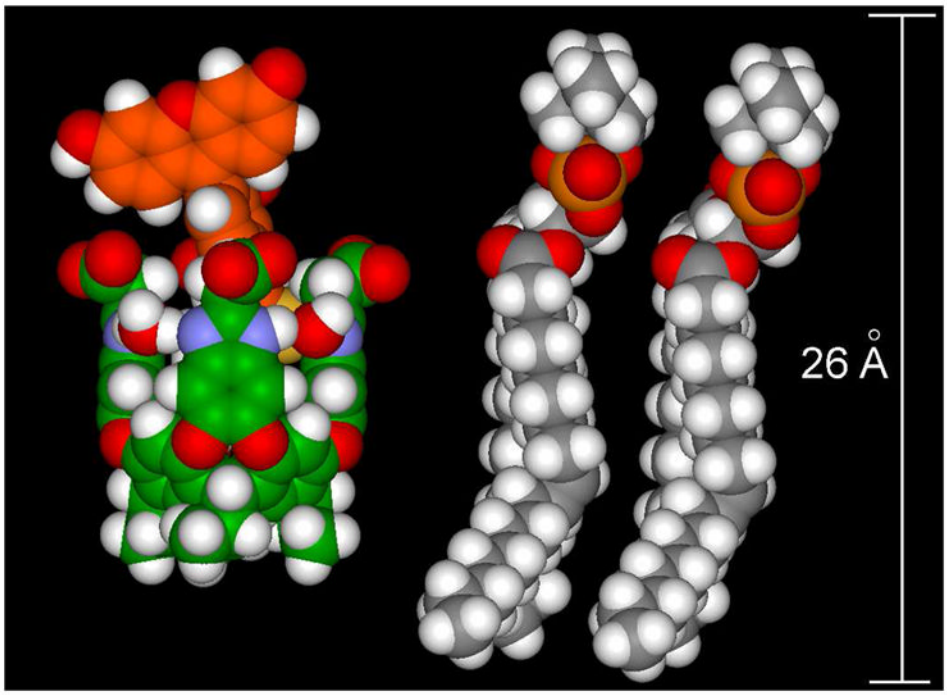

Figure 5.
Illustration of the relative sizes of the cavitand **1**·guest **6** complex and POPC lipids (host:guest complex minimized by SPARTAN, AM1 forcefield).

NIH-PA Author Manuscript

NIH-PA Author Manuscript

NIH-PA Author Manuscript

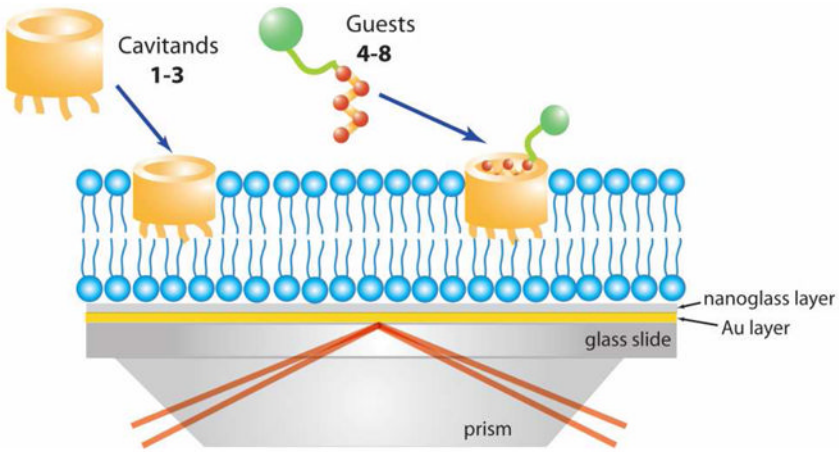

Scheme 1.

A cartoon representation of guests binding to cavitand **1** incorporated in a PC bilayer membrane.

NIH-PA Author Manuscript

NIH-PA Author Manuscript

NIH-PA Author Manuscript

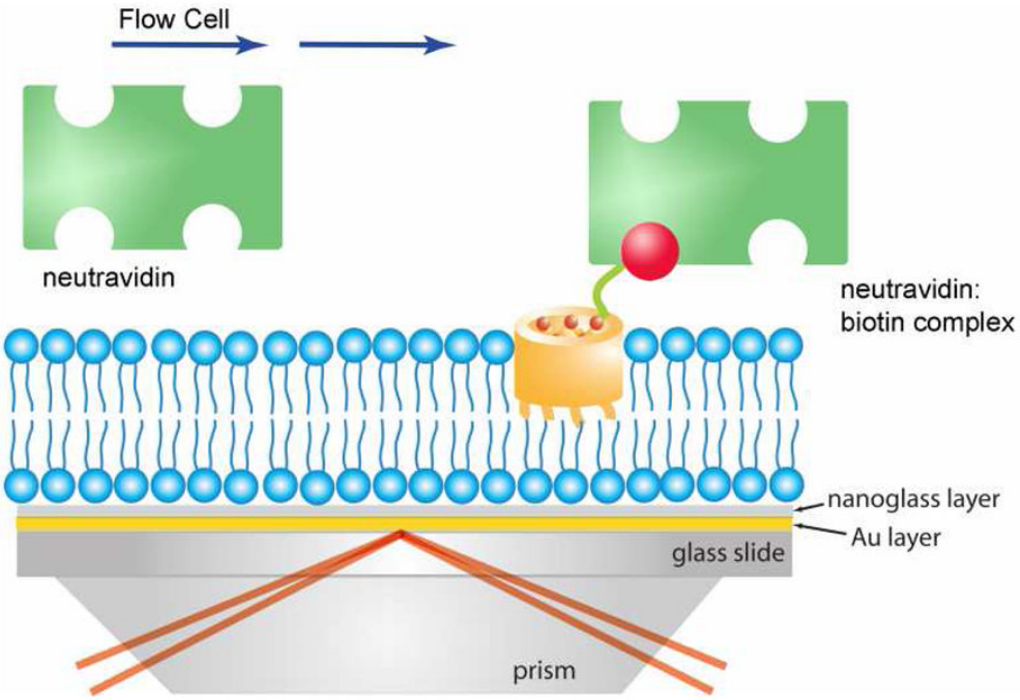

Scheme 2.

A cartoon representation of NeutrAvidin binding to the complex of cavitand **1** and guests **7** or **8** incorporated in a PC bilayer membrane.

NIH-PA Author Manuscript

NIH-PA Author Manuscript

NIH-PA Author Manuscript

Table 1

Binding properties of guest molecules **4**–**8** in the PC·**1** complex.

Guest	M_w	K_A/M^{-1}	K_d/mM
4	104.2	N/A	N/A
5	288.5	N/A	N/A
6	492.6	282 ± 73	3.54 ± 0.92
7	329.2	535 ± 68	1.87 ± 0.24
8	442.3	513 ± 160	1.95 ± 0.61